Metabolomics (2019) 15:32
https://doi.org/10.1007/s11306-019-1497-2

ORIGINAL ARTICLE

Selective galactose culture condition reveals distinct metabolic signatures in pyruvate dehydrogenase and complex I deficient human skin fibroblasts

Damian Hertig[1,2,3] · Andrea Felser[2] · Gaëlle Diserens[1] · Sandra Kurth[2] · Peter Vermathen[1] · Jean-Marc Nuoffer[2,4]

Received: 8 October 2018 / Accepted: 21 February 2019

Abstract

Introduction A decline in mitochondrial function represents a key factor of a large number of inborn errors of metabolism, which lead to an extremely heterogeneous group of disorders.

Objectives To gain insight into the biochemical consequences of mitochondrial dysfunction, we performed a metabolic profiling study in human skin fibroblasts using galactose stress medium, which forces cells to rely on mitochondrial metabolism.

Methods Fibroblasts from controls, complex I and pyruvate dehydrogenase (PDH) deficient patients were grown under glucose or galactose culture condition. We investigated extracellular flux using Seahorse XF24 cell analyzer and assessed metabolome fingerprints using NMR spectroscopy.

Results Incubation of fibroblasts in galactose leads to an increase in oxygen consumption and decrease in extracellular acidification rate, confirming adaptation to a more aerobic metabolism. NMR allowed rapid profiling of 41 intracellular metabolites and revealed clear separation of mitochondrial defects from controls under galactose using partial least squares discriminant analysis. We found changes in classical markers of mitochondrial metabolic dysfunction, as well as unexpected markers of amino acid and choline metabolism. PDH deficient cell lines showed distinct upregulation of glutaminolytic metabolism and accumulation of branched-chain amino acids, while complex I deficient cell lines were characterized by increased levels in choline metabolites under galactose.

Conclusion Our results show the relevance of selective culture methods in discriminating normal from metabolic deficient cells. The study indicates that untargeted fingerprinting NMR profiles provide physiological insight on metabolic adaptations and can be used to distinguish cellular metabolic adaptations in PDH and complex I deficient fibroblasts.

Keywords Galactose · Complex I · Pyruvate dehydrogenase · NMR · Mitochondrial dysfunction

Damian Hertig and Andrea Felser: shared first author.

Peter Vermathen and Jean-Marc Nuoffer: shared last author.

Electronic supplementary material The online version of this article (https://doi.org/10.1007/s11306-019-1497-2) contains supplementary material, which is available to authorized users.

✉ Jean-Marc Nuoffer
jean-marc.nuoffer@insel.ch

1 Departments of BioMedical Research and Radiology, University of Bern, Bern, Switzerland

2 Institute of Clinical Chemistry, Inselspital, University Hospital Bern, 3010 Bern, Switzerland

3 Graduate School for Cellular and Biomedical Sciences, University of Bern, Bern, Switzerland

4 Department of Paediatrics, Inselspital, University Hospital Bern, Bern, Switzerland

1 Introduction

Mitochondrial dysfunction is associated with a range of human pathologies that often appear as a consequence of defects in the oxidative phosphorylation (OXPHOS) (Koopman et al. 2012, 2013). These disorders manifest at any age and can impact virtually any organ system (DiMauro 2004; Mitochondrial Medicine Society's Committee et al. 2008). Subtle declines in OXPHOS are associated with skeletal muscle atrophy, neurodegeneration, and the aging process itself (Vafai and Mootha 2013). Metabolic consequences of OXPHOS defects are due to ATP shortage and increased free radicals. Both may have effects on a wide range of metabolic pathways and the cellular metabolome (Smeitink et al. 2006). The currently used diagnostic methods at metabolite, enzymatic or functional level in

Published online: 28 February 2019

body fluids or tissues are prone to misinterpretations and require further extensive clinical and laboratory evaluation (Smeitink 2003). There is nevertheless growing interest in rare mitochondrial disorders, and studying pathomechanism of OXPHOS dysfunction may shed light into the role of mitochondria in more common diseases.

It is well established that cells with oxidative defects frequently rely on ATP synthesis from glycolysis and are able to maintain normal growth rate in high glucose (GLC) containing media. However, severe growth impairment and increased rate of cell death occur when GLC is replaced by galactose (GAL) (Marroquin et al. 2007; Robinson et al. 1992). The non-viability of cells with oxidative defects in GAL medium is frequently used as a screening test for affected patient fibroblasts (FB) (Robinson et al. 1992). Under GAL condition, the slow metabolism of galactose to glucose-1-phosphate is not sufficient for the cells to cover their energy demand by glycolysis, and cells are forced to rely on OXPHOS for ATP synthesis. Cells grown in GAL are thus characterized by a decreased anaerobic glycolytic rate and an increased mitochondrial oxidative capacity as evidenced by increased OXPHOS protein expression and mitochondrial enzymatic activities over time (Aguer et al. 2011; Rossignol et al. 2004).

High-Resolution Magic Angle Spinning (HR-MAS) ^{1}H NMR spectroscopy has been established as a powerful tool for metabolic characterization of tissues and cell samples, and has been increasingly applied to identify metabolic changes associated with genetic modifications or drug treatments (Beckonert et al. 2010; Moestue et al. 2011; Morvan and Demidem 2018; Udhane et al. 2017; Vermathen et al. 2017). ^{1}H NMR spectroscopy is particularly appropriate for investigating metabolic compositions of biological samples as a wide range of metabolites involved in OXPHOS can be quantified simultaneously with no or simple sample preparation and without pre-selection bias (Nicholson et al. 1999). HR-MAS NMR based metabolome analysis may therefore be an ideal tool for investigating mitochondrial diseases.

In this study we investigate the metabolic adaption to GAL stress of two commonly defined mitochondrial defects, namely pyruvate dehydrogenase (PDH) and complex I (CI) deficiency. The mitochondrial PDH complex catalyzes the rate-limiting step in the aerobic GLC oxidation, while isolated CI deficiency is the most frequently observed mitochondrial respiratory chain disorder (Brown et al. 1994; Kirby et al. 1999; Loeffen et al. 2000; Robinson et al. 1996). We show that incubation in GAL-based media greatly improves discriminating normal from metabolic deficient cells and describe a metabolic signature consisting of 20 compounds that distinguish PDH or CI FB from controls. The metabolites provide insight into the metabolic pathway derangements that ensue from GAL stress and a valuable resource for understanding the biochemical consequences of mitochondrial dysfunction.

2 Materials and methods

2.1 Cell culture

Human FB cell lines were previously established from skin biopsies for diagnostic purposes. We studied FB derived from four controls, two patients with PDH deficiency (PDH1Eα defects, PDH activities 5.0 and 0.9 mAbs/mU citrate synthase activity (CS), reference 23–53 mAbs/mU CS), and two patients with CI deficiency (ND6 and NDUFAF2 defects; CI activities 0.14 and 0.11 mU/mU CS, respectively; reference range 0.19–0.46 mU/mU CS) (Suppl. Table 1). Six biological replicates were prepared for each cell line. Cells were maintained in minimal essential medium (Gibco, Carlsbad, CA) supplemented with 25 mM glucose, 10% foetal calf serum, 2 mM L-glutamine, 1 mM sodium pyruvate, 200 µM uridine, 1× non-essential amino acids (100 µM glycine, L-alanine, L-asparagine, L-aspartic acid, L-glutamic acid, L-proline, L-serine), 100 U/ml penicillin, 100 µg/ml streptomycin and 10 µg/ml chlortetracycline. FB were cultured at 37 °C in a humidified 5% CO_2 cell culture incubator and were passaged using 0.05% trypsin–EDTA. Cell numbers were determined in a Neubauer hemacytometer using trypan blue exclusion method. For metabolic investigations, cells were washed once with PBS and cultivated for 18 h in Dulbecco's Modified Eagle Medium (Gibco, Carlsbad, CA) supplemented with 5.5 mM GLC or 10 mM GAL, 10% dialyzed foetal calf serum, 2 mM L-glutamine, 1 mM sodium pyruvate, 1× nonessential amino acids, 200 µM uridine, 100 U/ml penicillin, 100 µg/ml streptomycin and 10 µg/ml chlortetracycline.

2.2 Bioenergetic analysis using Seahorse XF24 metabolic flux analysis

Cellular oxygen consumption rate (OCR) and extracellular acidification rate (ECAR) were investigated in unbuffered culture medium using a Seahorse XF24 cell analyzer (Agilent Technologies, CA, USA). FB were seeded in a density of 20′000 cells/well in XF24-well culture plates and allowed to adhere overnight. For each FB cell line, both culture conditions were evaluated in two independent experiments containing five replicates.

Medium was changed 18 h before the measurement to either GAL- or GLC-based medium after one washing step with PBS. One hour before the assay initiation, the medium was replaced with unbuffered medium and cells were equilibrated at 37 °C in a CO_2-free incubator. After the initial assessment of basal OCR and ECAR rates, sequential

exposures to modulators of mitochondrial function were injected. First, mitochondrial phosphorylation was inhibited by adding oligomycin (1 µM) to determine the oxidative leak, the mitochondrial electron transport chain was titrated to maximal respiration by the addition of the uncoupler carbonyl cyanide-*p*-trifluoromethoxyphenylhydrazone (2 µM FCCP, followed by 0.5 µM), and finally non-mitochondrial respiration was determined after the addition of the combined injection of rotenone (1 µM, CI inhibitor) and antimycin A (0.5 µM, complex III inhibitor). Cell numbers in each well were assessed after each experiment using the CyQuant assay (Thermo Fisher Scientific, Carlsbad, CA) and values were normalized to corresponding cell numbers. For the calculation of specific steady-states, OCR was additionally corrected for non-mitochondrial oxygen consumption. Maximal respiration is defined as OCR under FCCP, while maximal acidification corresponds to ECAR under oligomycin.

2.3 NMR spectroscopy

Cells were seeded to a 150 cm^2 tissue culture flask in a density of 2.2 million cells per flask. Cell pellets for NMR analysis were prepared following a protocol that was established previously (Diserens et al. 2017). After treatment, cells were collected and washed three times with 1 ml PBS. Next, cells were suspended in 60 µl D_2O based 10 mM PBS (pH 7.4), sonicated for 30 s in a ultrasonic bath at 50 Kc and shock-frozen using liquid nitrogen in three cycles. Finally, cell metabolism was inactivated by heating the sample at 70 °C for 20 min (Diserens et al. 2017). The cell suspension was transferred into a standard zirconium magic angle spinning rotor using a 50 µl insert. For each culture condition (GLC or GAL), three independent samples were prepared for each cell line, corresponding to 48 independent biological replicates (8 cell lines × 2 media × 3 samples).

The ^{1}H HR-MAS NMR experiments were performed on a 500 MHz Bruker Avance II spectrometer (Bruker BioSpin). The instrument is equipped with a 4 mm HR-MAS dual inverse 1H/13C probe (Bruker BioSpin) with a magic angle gradient. All HR MAS NMR experiments were carried out at a magic angle (54.7°) spinning rate of 3 kHz at a nominal temperature of 279 K. The Bruker Topspin software (version 3.2, patch level 5) was used to acquire the NMR data.

A 1D ^{1}H T2-filter sequence eliminating J-modulation ("project") with water presaturation was used in this study (Aguilar et al. 2012). This sequence has been shown to efficiently replace the well-known CPMG sequence also in biopsy measurements, with the advantage of reducing the J-evolution due to the addition of a 90° pulse between the 180° pulses of the traditional CPMG sequence.

For each FB sample, three 1D project spectra of 256 transients each were measured. The three project spectra were measured using following parameters: a spectral width of 6009.615 Hz, a data size of 32 K points, an acquisition time of 2.73 s and a relaxation delay of 4 s. A rotor synchronized T_2-filter of 211 ms was applied to suppress broad components with short T_2 relaxation times. The 90° pulse length was optimized for each sample. For selected samples, phase-sensitive 2D ^{1}H^{1}H-TOCSY spectra using the DIPSI sequence ("dipsi2phpr" from the Bruker pulse program library) with water presaturation were recorded to help spectral assignment.

For all spectra, the co-added free induction decays were exponentially weighted with a line broadening factor of 1.0 Hz, Fourier-transformed, manually phased, baseline corrected and frequency calibrated to the left peak of the lactate doublet (1.324 ppm) to obtain the ^{1}H NMR spectra. Spectral assignments was done using literature reference (Vermathen et al. 2015), our own additional 2D correlation spectroscopy (^{1}H^{1}H-TOCSY) measurements and comparison with reference spectral databases [own and the Human Metabolome Database (Wishart et al. 2013)].

A total of 115 buckets (between 0.8 and 9.4 ppm) were selected, with a variable size according to the peak width. Spectral regions comprising only noise were excluded from all analyses. To account for differences in cell pellet volumes the buckets were normalized by probabilistic quotient normalization (Dieterle et al. 2006), which has been shown to be a robust normalization technique, and scaled with unit variance scaling. After assigning the signals to metabolites, correlating signals ($r > 0.6$) at different spectral regions originating from the same metabolite were merged, yielding a metabolic profile including specific values of 41 different metabolites. Individual peak analysis was performed with MatLab (R2014b, The MathWorks Inc.) and PLS_Toolbox (Eigenvector Research, Inc.). Partial Least Squares Discriminant Analyses (PLS-DA) were performed to compare the 41 metabolite contents of healthy control, PDH deficient, and CI deficient FB.

HR-liquid state NMR experiments of culture media samples were performed with a 5 mm ATM BBFO probe with z-gradient. Following a waiting time of at least 600 s for temperature equilibration, each spectrum was acquired using the 1D PROJECT pulse sequence with water presaturation and a T_2-filter of 80 ms. All spectra were measured using the same parameters: a nominal temperature of 277 K, a spectral with of 10,000 Hz, a data size of 64 K points, 128 transients, an acquisition time of 3.28 s and a relaxation delay of 5 s. Phased and baseline corrected ^{1}H NMR spectra were calibrated to the TSP resonance (0 ppm) which was used as an internal reference. For the HR-liquid state NMR measurements of the media, a total of 36 assigned buckets with a variable size were assigned and summarized as described above, yielding a profile including values of 17 compounds of GLC or GAL medium. No normalization was necessary for the buckets

from supernatant spectra. Artificial results due to differences in media and spectra affecting the normalization were thus avoided.

2.4 Statistics

Statistical analyses were performed using GraphPad Prism 5 (GraphPad Software, La Jolla, CA, USA). For evaluation of extracellular flux analysis, we performed two-way analysis of variance (ANOVA) followed by a Bonferroni post-test. p Values < 0.05 were considered significant. The metabolites obtained from NMR measurements were examined by two-way ANOVA followed by Benjamini and Hochberg post-test, using a false discovery rate of 0.25. p Values < 0.01 were considered significant.

3 Results

3.1 GAL enhances oxidative metabolism and reveals distinct bioenergetic adaptations in PDH and CI deficient FB

We analyzed metabolic flux by direct assessment of the oxygen consumption rate (OCR) and extracellular acidification rate (ECAR) in intact cells. Incubation of control FB in GAL lead to an increase of basal and maximal OCR, confirming their adaptation to a more aerobic metabolism (Fig. 1a, c). PDH deficient cells adapted their basal OCR under GAL to a higher level than controls, while reaching the same maximal OCR. In contrast, CI deficient cells failed to increase OCR, and were characterized by a lower maximal OCR under GLC and GAL condition. ECAR was decreased under GAL in all cell lines, confirming slower glycolytic flux. PDH deficient cells showed increased basal ECAR in GLC compared to

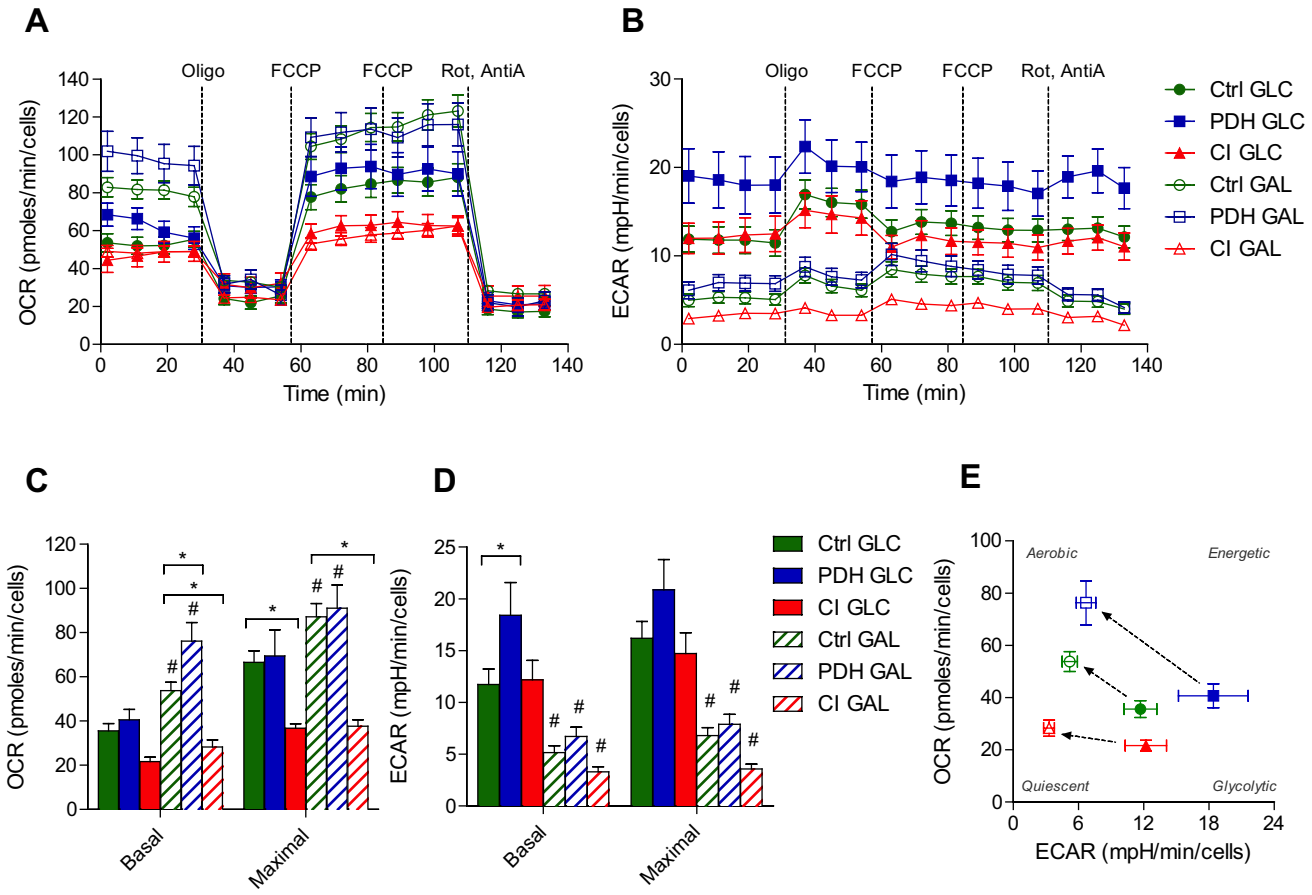

Fig. 1 Metabolic flux analysis. **a**, **b** Oxygen consumption rate (OCR) and extracellular acidification rate (ECAR) were measured over time after sequential addition of different modulators of mitochondrial function. **c**, **d** Quantitative analysis of basal and maximal steady-states of OCR and ECAR. **e** Bioenergetic profiling under basal condition. Values represent the mean ± SEM. Statistical significance between groups was calculated by two-way ANOVA followed by Bonferroni posttest. *p < 0.05, Ctrl versus PDH or CI in each culture condition; #p < 0.05, GLC versus GAL for Ctrl, PDH or CI

controls, whereas no differences were observed in CI deficient cells (Fig. 1b, d). Finally, the shift in energy phenotype from GLC to GAL based media led to a clear separation of PDH, CI and control cell lines (Fig. 1e). While PDH deficient FB shifted towards a more aerobic phenotype, CI deficient FB switched to an almost quiescent phenotype. Importantly, the analyzed 18 h exposure to GLC and GAL based medium had no significant effect on cell proliferation in Ctrl, PDH or CI deficient cells, excluding a differential effect on cell survival (Supplementary Fig. 1).

3.2 Chemometric analysis of intracellular metabolites in PDH and CI deficient FB reveals metabolomic separation under GAL

Resonances of the NMR spectra were assigned to overall 41 intracellular metabolites (Fig. 2; Table 1). Under GLC, principal component analysis (PCA) of intracellular metabolites did not demonstrate any separation between control, PDH and CI deficient FB (Fig. 3a). Partial least squares discriminant analysis (PLS-DA) revealed significant separation of control and PDH defects under GLC, while CI deficient FB were not significantly separated from controls (Fig. 3b). In contrast, under GAL the intracellular metabolomes of control, PDH and CI deficient FB were already separated in unsupervised PCA (Fig. 3c). Supervised PLS-DA yielded complete separation of all three groups (all $p < 0.05$ based on permutation test, $Q^2 > 0.64$) (Fig. 3d), indicating a distinct metabolic profile in patients and controls. CI and PDH were principally separated from controls along the latent variable 1 (LV1), with strongest influence on the separation of the metabolites creatinine and fumarate. PDH was mainly separated from CI and controls along LV2, with strongest influence on the separation of the metabolites choline and phenylalanine (loading plots shown in Supplementary Fig. 2).

3.3 Analysis of individual metabolites shows specific defect dependent differences in GLC and GAL based media

We found twenty intracellular metabolites significantly changed (complete list of intracellular metabolites in Table 1). Four metabolites are key substrates or intermediate compounds of TCA cycle and glucose metabolism,

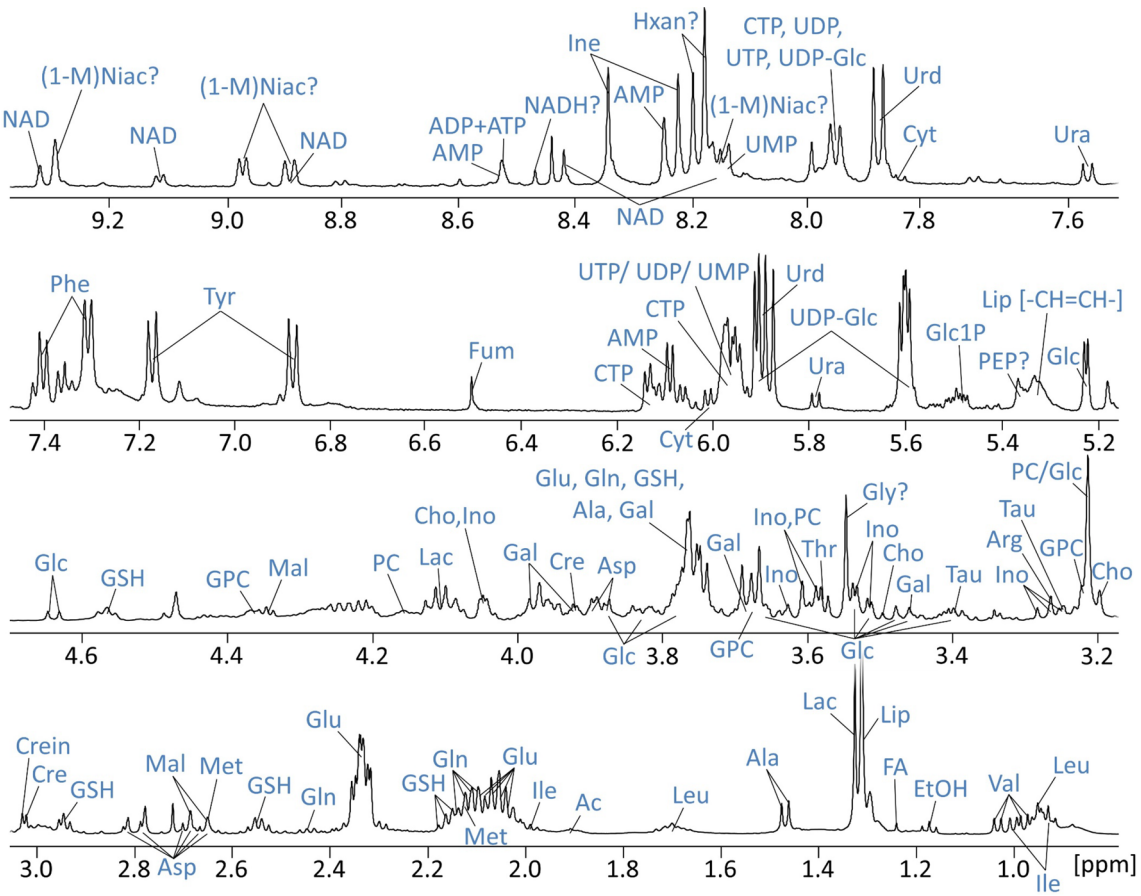

Fig. 2 Summed ^{1}H HR-MAS NMR spectrum with assignments of selected metabolites identified in cell lysates of fibroblasts. Metabolites labeled with "?" require further confirmation. All the metabolite abbreviations used in this figure are listed in Tables 1 and 2

Table 1 Complete list of integrated buckets of ^{1}H HR-MAS NMR resonances of intracellular metabolites in lysed cell pellets of Ctrl, PDH, and CI deficient fibroblasts under GLC or GAL culture condition

Intracellular metabolites	GLC						GAL					
	Ctrl mean	± SD	PDH mean	± SD	CI mean	± SD	Ctrl mean	± SD	PDH mean	± SD	CI mean	± SD
1-Methyl niacinamide (1M-Niac)?	0.9	± 0.3	1.1	± 0.1	1.7*	± 0.5	1.0	± 0.2	1.4*#	± 0.2	2.1*#	± 0.4
ADP+ATP	1.8	± 1.1	1.6	± 0.7	1.4	± 0.8	1.8	± 1.1	2.1	± 0.8	1.4	± 0.7
Alanine (Ala)	14.1	± 1.8	14.1	± 0.9	13.3	± 1.5	16.2#	± 3.6	16.1#	± 0.2	14.7	± 1.7
Arginine (Arg)	2.7	± 1.8	2.2	± 0.6	3.1	± 1.1	2.9	± 2.4	2.4	± 1.0	2.9	± 0.6
Aspartate (Asp)	1.3	± 0.3	1.4	± 0.1	0.9	± 0.2	2.8#	± 0.8	3.5#	± 0.8	3.7#	± 1.4
Choline (Cho)	5.4	± 1.1	3.1*	± 0.5	7.7*	± 0.8	4.6	± 1.2	3.1	± 0.5	9.2*	± 1.4
Creatine (Cre)	4.6	± 1.2	5.4	± 0.5	5.9	± 0.7	3.7	± 1.2	4.6	± 1.1	4.7	± 1.1
Creatinine (Crein)	3.6	± 1.2	4.7	± 0.4	4.8	± 0.3	2.3#	± 0.5	3.9*	± 0.4	4.4*	± 0.3
Cytidine (Cyt)	0.3	± 0.3	0.3	± 0.3	0.1	± 0.0	0.1	± 0.1	0.4	± 0.5	0.1	± 0.2
FA (CH2)n chain	5.8	± 0.5	5.7	± 0.3	5.5	± 0.4	5.4	± 0.7	5.7	± 0.7	4.9	± 0.7
Fatty acid (FA)	3.0	± 2.5	4.2	± 3.1	3.0	± 1.4	2.9	± 2.7	5.5	± 4.5	2.8	± 1.5
Fumaric acid (Fum)	0.2	± 0.1	0.2	± 0.1	0.1*	± 0.1	0.6#	± 0.2	0.4*#	± 0.1	0.4*#	± 0.1
Glucose-1-phosphate (Glc1P)	0.3	± 0.3	0.3	± 0.1	0.3	± 0.2	1.7#	± 0.6	2.2	± 1.4	1.4	± 0.5
Glutamate (Glu)	102.1	± 9.8	97.1	± 4.8	95.6	± 6.6	85.3	± 9.2	78.2	± 9.8	85.8	± 11.4
Glutamine (Gln)	2.4	± 1.1	1.3	± 1.2	3.4	± 1.6	6.9	± 4.8	8.1#	± 0.6	10.0	± 6.3
Glycerophosphocholine (GPC)	6.5	± 1.5	2.9*	± 0.1	5.6	± 1.2	4.1#	± 0.8	2.9*	± 0.5	4.8	± 1.0
Glycine? (Gly)	12.9	± 3.0	17.2	± 4.2	14.9	± 2.6	13.4	± 2.6	15.7	± 2.2	14.1	± 1.0
Glutathione (GSH)	10.8	± 1.5	8.3*	± 1.6	8.3*	± 1.4	9.6	± 0.9	8.4	± 2.0	8.9#	± 0.9
Hypoxanthine? (HXan)	2.6	± 0.7	2.7	± 0.6	2.7	± 0.3	3.0	± 0.6	2.7	± 0.3	2.7	± 0.5
Inosine (Ine)	3.0	± 0.9	2.7	± 0.8	2.6	± 0.6	3.2	± 1.2	2.6	± 1.2	2.5	± 0.3
Inositol (Ino)	4.8	± 1.5	4.8	± 0.6	5.5	± 1.4	4.2	± 1.7	4.5	± 0.5	4.3	± 1.5
Isoleucine (Ile)	7.1	± 0.9	8.7*	± 0.3	7.9	± 0.8	6.4	± 0.8	7.9*	± 0.6	6.4	± 0.9
Lactic acid (Lac)	32.8	± 5.4	33.0	± 4.2	28.7	± 3.4	35.1	± 5.9	37.4	± 6.5	24.3*	± 2.7
Leucine (Leu)	19.3	± 2.2	23.4*	± 0.9	21.4	± 2.0	17.1	± 1.9	21.0*	± 1.1	17.2	± 2.1
Lipid (Lip) [–(CH2)n–]	10.4	± 2.5	11.3	± 2.8	13.1	± 3.9	12.6	± 3.4	15.2	± 6.7	15.1	± 3.3
Lipid (Lip) [–CH=CH–]	3.3	± 2.3	4.9	± 1.4	2.8	± 1.8	2.4	± 1.7	4.7	± 2.3	4.2	± 3.1
Lipid (Lip) [CH2 lysyl protein]	12.5	± 1.4	11.6	± 0.3	11.4	± 1.4	11.2	± 1.3	11.3	± 0.9	10.5	± 1.0
Lipid (Lip) [ω-CH3]	14.4	± 2.2	14.2	± 2.5	12.6	± 2.2	13.4	± 1.9	14.7	± 4.9	12.5	± 2.2
NAD	0.6	± 0.2	0.5	± 0.2	0.4	± 0.2	0.7	± 0.2	0.6	± 0.2	0.6	± 0.2
NADH?	0.3	± 0.2	0.3	± 0.2	0.3	± 0.2	0.4	± 0.2	0.4	± 0.3	0.3	± 0.2
Phosphocholine (PC)	16.8	± 2.7	12.7*	± 1.0	22.6*	± 3.4	14.7	± 2.6	14.4	± 1.5	24.9*	± 5.2
Phenylalanine (Phe)	5.1	± 0.5	6.0*	± 0.3	5.5	± 0.2	4.5	± 0.4	5.6*	± 0.3	4.6	± 0.4
Phosphoenolpyruvate? (PEP)	0.9	± 0.4	1.1	± 0.2	0.9	± 0.2	1.1	± 0.4	1.3	± 0.3	0.9	± 0.2
Taurine (Tau)	0.8	± 0.3	0.7	± 0.1	1.3*	± 0.1	0.8	± 0.3	0.6	± 0.1	1.4*	± 0.1

Table 1 (continued)

Intracellular metabolites	GLC					GAL				
	Ctrl mean	± SD	PDH mean	± SD	CI mean	± SD	Ctrl mean	± SD	PDH mean	± SD	CI mean	± SD
Threonine (Thr)	3.9	± 1.0	4.6	± 0.6	4.3	± 0.8	2.5#	± 0.6	3.1#	± 0.3	2.6#	± 0.4
Tyrosine (Tyr)	4.1	± 0.6	5.1*	± 0.3	4.5	± 0.5	3.5#	± 0.5	4.5*	± 0.5	3.6#	± 0.2
UDP Glucose (UDPGlc)	7.9	± 1.9	6.9	± 1.0	7.0	± 0.8	8.0	± 1.8	6.4	± 0.8	6.2	± 1.0
UMP	2.6	± 0.4	2.2	± 0.3	2.3	± 0.1	2.7	± 0.5	2.6	± 0.2	2.7	± 0.5
Uracil (Ura)	0.8	± 0.8	0.5	± 0.3	0.7	± 0.4	0.9	± 1.2	0.5	± 0.6	0.4	± 0.2
Uridine (Urd)	5.8	± 1.8	5.0	± 1.3	4.8	± 1.0	4.8	± 1.6	3.4	± 0.7	3.0	± 0.6
Valine (Val)	6.4	± 1.0	8.4*	± 0.6	7.7	± 1.1	5.7	± 0.9	7.8*	± 0.7	6.1	± 1.0

Values represent the mean ± SD in normalized arbitrary units. Statistical significance between groups was calculated by two-way ANOVA followed by Benjamini and Hochberg posttest

Ctrl control, *PDH* pyruvate dehydrogenase, *CI* complex I

"?" Metabolite identification needs further confirmation

*$p < 0.01$, Ctrl versus PDH or CI in each culture condition

#$p < 0.01$, GLC versus GAL for Ctrl, PDH or CI

i.e. fumarate, glutamine, glucose-1-phosphate, and lactate (Fig. 4a). Although ECAR was decreased in all cell lines under GAL, we found an intracellular decrease of lactate in CI deficient cells only. However, additional assessment of extracellular metabolites in culture medium revealed about 4 to fivefold lower lactate under GAL for all FB groups, confirming decreased basal ECAR in the metabolic flux analysis (complete list of extracellular metabolites in Table 2).

We found specific perturbations in intracellular amino acid metabolic pathways, such as changes in alanine, aspartate, and threonine (Fig. 4b). Interestingly, we found a PDH-deficiency related increase of all branched-chain amino acids, namely isoleucine, leucine, and valine, as well as an increase of the aromatic amino acids phenylalanine and tyrosine under GLC and GAL culture conditions. Other amino acid derivatives were altered also, such as creatinine, taurine, and glutathione (Fig. 4c). Additionally, we found specific alterations in choline metabolites, such as choline, phosphocholine, and glycerophosphocholine (Fig. 4d). While levels of choline containing metabolites were increased in CI deficient FB, they were decreased in PDH deficient FB. We also observed changes in other metabolites such as 1-methyl-niacinamide and uridine (Fig. 4e).

4 Discussion

In this study, we investigated GAL-induced stress in two different mitochondrial disorders using a combined metabolic flux and NMR approach. Despite a small sample size, the current study design led to an improved discrimination between normal and metabolic deficient cells and enabled the identification of distinct metabolic signatures, consisting of upregulated aerobic metabolism and glutamine dependence, as well as altered amino acid and choline metabolism.

4.1 Markers of increased aerobic metabolism and glutamine dependence

Metabolic flux analysis revealed significant increase of mitochondrial OCR for control and PDH deficient cells under GAL, while as expected, CI deficient cell lines were not able to increase aerobic metabolism due to their defect in mitochondrial OXPHOS. Glucose-1-phosphate was increased in controls under GAL, which can be derived from metabolism of galactose (Robinson et al. 1992). At the same time ECAR and extracellular lactate were decreased in all cell lines under GAL, indicating a slower glycolytic flux under GAL.

It is known that limitation of GLC flow to the TCA cycle is associated with enhanced glutamine metabolism and is leading to glutamine-dependent cell survival (Li et al. 2016; Yang et al. 2014). Control and PDH deficient cells might alternatively fuel OXPHOS by glutaminolysis and therefore

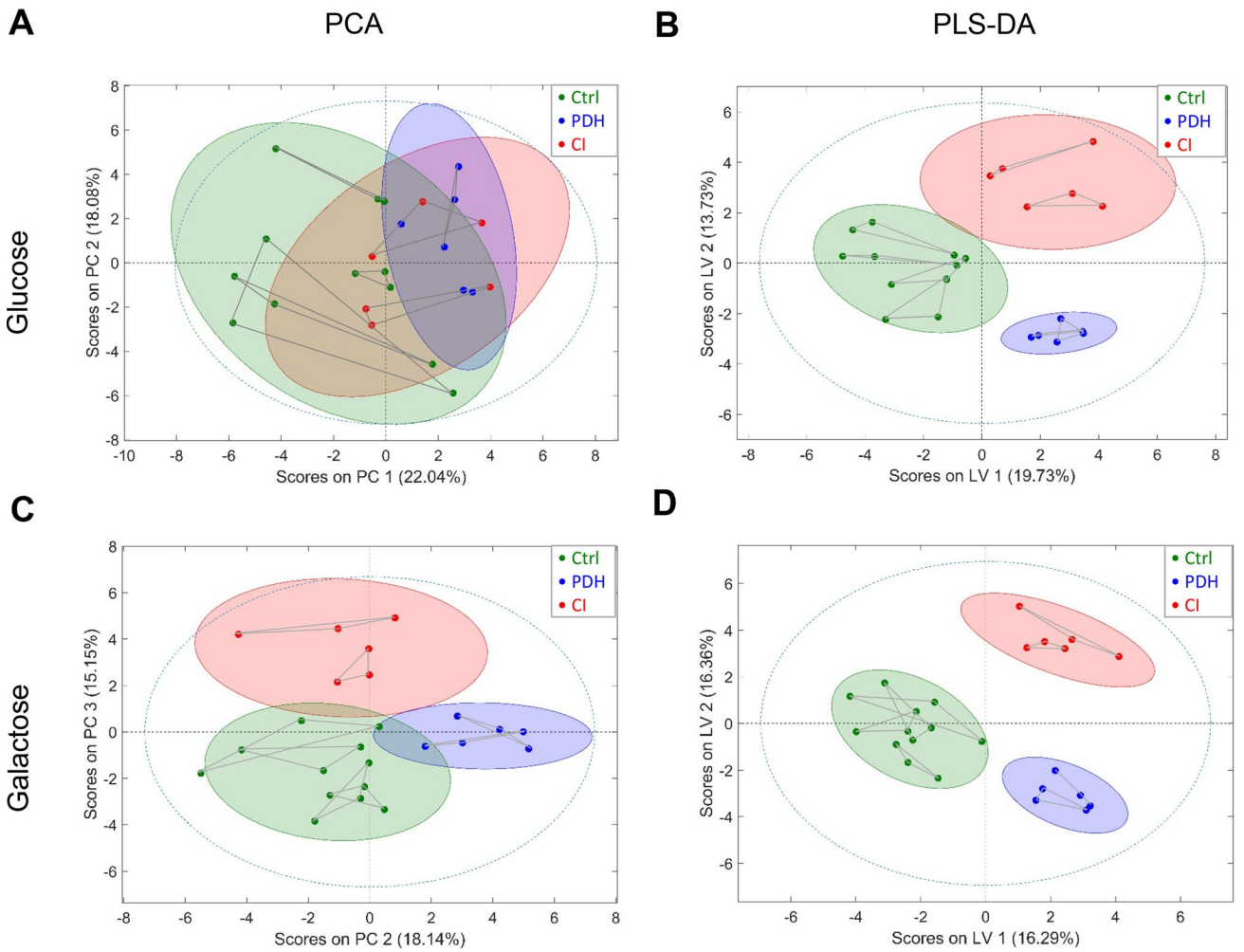

Fig. 3 Chemometric analysis. **a**, **c** Unsupervised principle component analysis (PCA) of GLC and GAL condition, respectively. **b**, **d** Supervised partial least squares discriminant analysis (PLS-DA) of GLC and GAL condition, respectively. Connecting lines represent biological replicate samples from the same cell line. Ellipsoids correspond to an 83% confidence interval. Cross validated rand t-test values obtained from permutation tests for PLS-DA: in GLC $p < 0.05$ for Ctrl, PDH, not significant for CI; in GAL $p < 0.05$ for Ctrl, PDH, and CI

increase their basal OCR. We found significant increase in intracellular glutamine levels in PDH deficient cells under GAL, which plays an important role in driving glucose-independent anaplerotic needs to the TCA cycle. Furthermore, the accumulation of intracellular aspartate and alanine might result from increased transaminase activities for maintaining anaplerotic metabolism via glutaminolytic pathway (Yang et al. 2014).

4.2 Perturbations in amino acid metabolic pathways

Branched-chain amino acids (BCAA), including leucine, isoleucine and valine, are essential amino acids for mammals and were increased in PDH deficient cells under GLC and GAL. Key mechanisms in governing BCAA homeostasis are their uptake or catabolism, as well as the rate of protein turnover (Harper et al. 1984). BCAA are first converted into branched-chain alpha-ketoacids and eventually metabolized via acetyl-CoA as well as succinyl-CoA for oxidation in the TCA cycle. The rate-limiting enzyme of this pathway, branched-chain α-ketoacid dehydrogenase complex, has a shared enzymatic subunit E3 with the PDH complex (Johnson et al. 2000). However, the PDH deficient FB had no mutation within this subunit. Accumulations of BCAA are also known to be involved in metabolic signalling (Li et al. 2017; Lynch and Adams 2014), and play a role as allosteric activators of glutamate dehydrogenase (Mastorodemos et al. 2005; Zhou and Thompson 1996). Further investigations are necessary in order to elucidate the association between PDH defects and amino acid dysmetabolism.

Table 2 Complete list from integrated buckets of ^{1}H HR-MAS NMR resonances of extracellular metabolites (in arbitrary units) in culture supernatant of Ctrl, PDH, and CI deficient fibroblasts under GLC or GAL culture condition

GLC supernatant	GLC medium	Ctrl mean	± SD	PDH mean	± SD	CI mean	± SD
Nicotinamide	0.6	0.6	± 0.2	0.7	± 0.1	0.6	± 0.2
Folic acid? Formic acid?	0.3	0.8	± 0.1	0.8	± 0.2	0.6	± 0.2
Uridine + cytidine	1.5	3.1	± 0.3	3.0	± 0.2	3.1	± 0.2
Uracil	1.7	1.8	± 0.9	1.5	± 0.4	1.2	± 0.6
Phenylalanine	9.6	12.6	± 0.6	12.5	± 0.6	12.8	± 0.5
Tyrosine	16.6	17.3	± 0.6	16.8	± 0.9	17.4	± 0.6
Glycerophosphocholine	0.6	3.0	± 0.5	3.6	± 0.4	3.4	± 0.3
Inositol	10.8	12.0	± 0.5	11.6	± 0.7	12.1	± 0.6
Aspartate	6.0	6.7	± 0.4	6.5	± 0.2	6.6	± 0.2
Glutamine	17.4	14.4	± 3.5	12.8	± 1.6	14.2	± 3.8
Glutamate, pyruvic acid	23.7	17.4	± 2.6	16.8	± 2.2	17.0	± 3.4
Alanine	17.2	20.4	± 1.9	19.4	± 1.0	19.9	± 1.9
Lactate	6.3	80.1	± 16.7	80.2	± 23.2	71.3	± 5.9
Isoleucine	20.6	20.3	± 0.8	19.8	± 1.3	21.0	± 0.8
Valine	20.6	20.3	± 0.8	19.7	± 1.1	21.0	± 0.9
Leucine	37.4	34.4	± 1.7	33.4	± 2.1	35.4	± 2.0
Glucose	31.3	25.9	± 2.0	24.6	± 3.7	26.2	± 2.5
GLC supernatant	GLC medium	Ctrl mean	± SD	PDH mean	± SD	CI mean	± SD
Nicotinamide	0.7	0.6	± 0.1	0.5	± 0.1	0.5	± 0.2
Folic acid? formic acid?	0.1	1.0	± 0.1	1.0	± 0.3	0.8	± 0.1
Uridine + cytidine	1.2	3.2	± 0.5	3.3	± 0.3	3.1	± 0.4
Uracil	0.0	2.2	± 1.1	2.0	± 0.5	1.9	± 0.6
Phenylalanine	9.7	13.0	± 0.8	12.6	± 1.0	12.8	± 0.9
Tyrosine	16.9	17.7	± 0.8	17.0	± 1.2	17.3	± 0.9
Glycerophosphocholine	0.1	3.1	± 0.6	3.7	± 0.4	3.4	± 0.6
Inositol	13.0	13.5	± 0.7	12.6	± 0.9	13.1	± 1.0
Aspartate	6.6	6.9	± 0.5	6.4	± 0.4	6.5	± 0.5
Glutamine	18.3	13.8	± 4.0	11.8	± 2.0	13.7	± 4.0
Glutamate, pyruvic acid	25.7	15.3	± 3.9	15.7	± 3.3	15.2	± 3.8
Alanine	18.4	19.4	± 2.1	18.7	± 1.2	19.0	± 1.8
Lactate	6.9	23.5	± 9.0	28.4	± 5.7	24.6	± 9.7
Isoleucine	22.0	21.1	± 1.1	20.1	± 1.8	20.9	± 1.2
Valine	21.7	21.1	± 1.1	20.2	± 1.7	21.1	± 1.2
Leucine	39.8	36.1	± 2.0	33.9	± 2.9	35.6	± 1.7
Galactose	50.8	52.1	± 2.9	49.5	± 4.4	50.1	± 3.5

Statistical significance between groups was calculated by two-way ANOVA followed by Benjamini and Hochberg posttest

"?" Metabolite identification needs further confirmation

Ctrl control, *PDH* pyruvate dehydrogenase, *CI* complex I

*$p < 0.01$, Ctrl versus PDH or CI in each culture condition

#$p < 0.01$, GLC versus GAL for Ctrl, PDH or CI

4.3 Disturbances in pathways related to choline metabolism

Other unexpected findings were increased levels of choline and phosphocholine in CI deficient FB and decreased choline metabolites in PDH deficient FB. Changes in choline metabolite levels might indicate altered turnover of membrane phospholipids, which are essential components of the plasma membrane and membranes of cellular organelles (Bluml et al. 1999). It is known that altered choline metabolic pathways might be associated with mitochondrial respiratory chain disorders (Baykal et al. 2008; Gropman 2013; Jansen et al. 1996). Complex I disorders are indeed associated with increased reactive oxygen species, which can

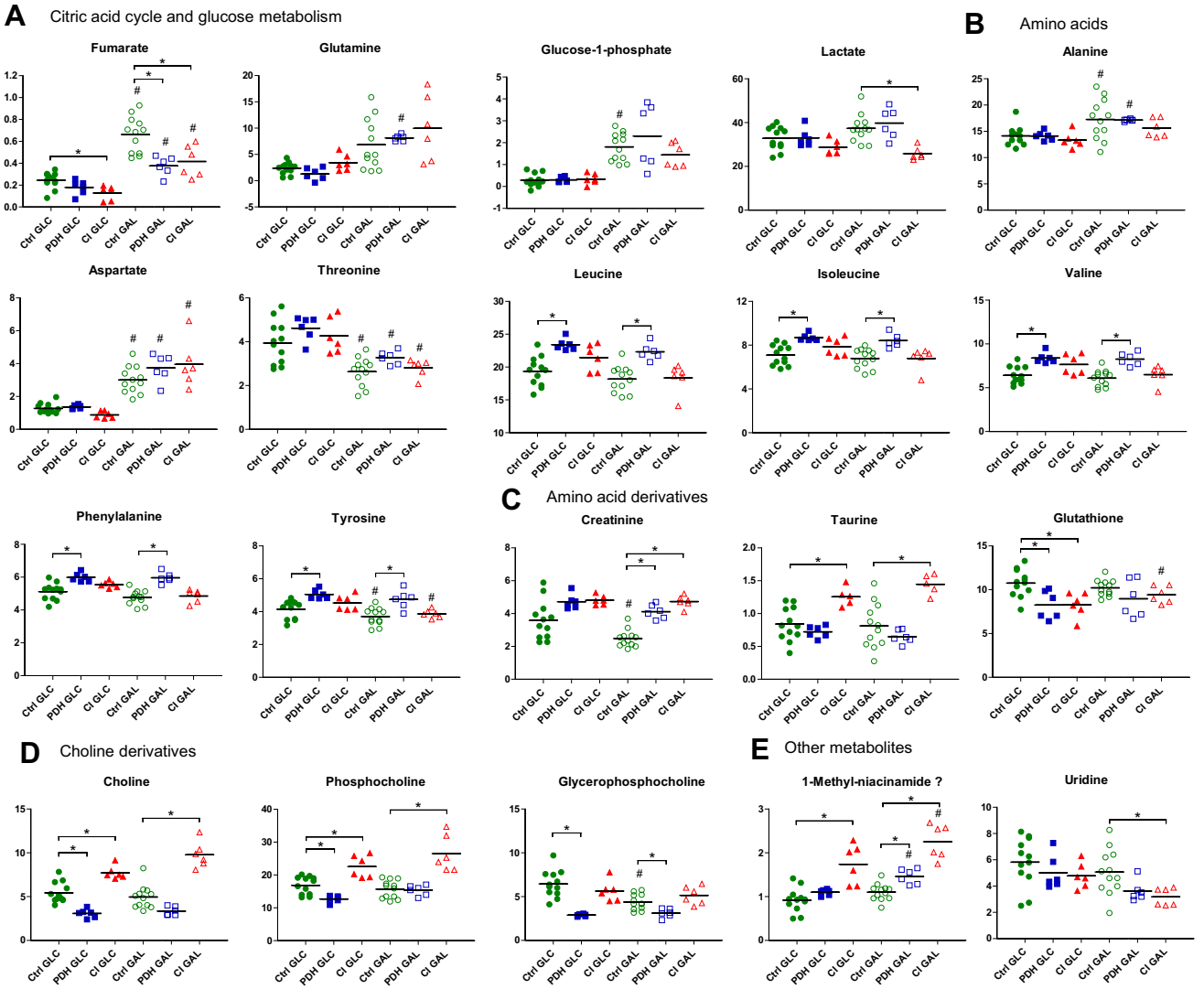

Fig. 4 Quantitative analysis of intracellular metabolites using ^{1}H HR-MAS NMR. Ctrl, PDH and CI fibroblasts were grown in GLC or GAL medium. In total, 41 metabolites were identified (see Table 1). **a**–**f** Summary of selected metabolites from NMR measurements showing significant alterations. Y-axis represents metabolite content in normalized arbitrary unit. Statistical significance between groups was calculated by two-way ANOVA followed by Benjamini and Hochberg posttest. *$p < 0.01$, Ctrl versus PDH or CI in each culture condition; $^{\#}p < 0.01$, GLC versus GAL for Ctrl, PDH or CI. "?", metabolite identification needs further confirmation

in turn induce increased membrane peroxidation (Robinson 1998). In agreement with this hypothesis we found increased levels of the antioxidant taurine and decreased glutathione in CI deficient FB. Altered choline catabolic and anabolic pathways might thus represent interesting potential biomarkers for mitochondrial dysfunction.

4.4 Conclusions

This study shows the relevance of selective culture methods in discriminating normal from metabolic deficient cells. Results uncovered specific cellular metabolic adaptations in PDH and CI defects, which have implications for understanding potential contributors of mitochondrial dysfunction and collectively highlight the complexity of perturbations that may result from mitochondrial dysfunction. Untargeted fingerprinting NMR profiles provide physiological insight on metabolic adaptations and can be used to distinguish specific mitochondrial diseases. Further studies will be needed in order to delineate the underlying metabolic mechanisms in more detail and characterize whether the identified metabolites may be relevant as biological markers in the two studied defects or other inherited mitochondrial disorders.

Acknowledgements We thank André Schaller (Division of Human Genetics and Department of Paediatrics, Inselspital, Bern) for providing the genetic characteristics of the patient fibroblasts.

Author contribution DH, AF, GD, SK, PV, and JMN conceived the work and designed the experiments; DH, AF, and SK cultured cells, performed metabolic flux experiments and analyzed the data. DH and GD performed NMR analysis of cells or supernatant and analyzed the data. PV and JMN provided experimental advice and overall guidance. DH, AF, GD, SK, PV and JMN wrote the manuscript or revised it critically for important intellectual content. All authors approved the final manuscript.

Funding This work was supported by a grant from the Batzebär foundation of the children's university hospitals Bern to JMN.

Compliance with ethical standards

Conflict of interest The authors have declared no conflicts of interest.

Ethical approval All procedures performed in studies involving human participants were in accordance with the 1964 Helsinki declaration and its later amendments and approved by the Ethics Committee of the University Hospital of Bern.

Informed consent Informed consent was obtained from all individual participants included in the study.

References

Aguer, C., et al. (2011). Galactose enhances oxidative metabolism and reveals mitochondrial dysfunction in human primary muscle cells. *PLoS ONE, 6*, e28536. https://doi.org/10.1371/journal.pone.0028536.

Aguilar, J. A., Nilsson, M., Bodenhausen, G., & Morris, G. A. (2012). Spin echo NMR spectra without J modulation. *Chemical Communications (Camb), 48*, 811–813. https://doi.org/10.1039/c1cc16699a.

Baykal, A. T., Jain, M. R., & Li, H. (2008). Aberrant regulation of choline metabolism by mitochondrial electron transport system inhibition in neuroblastoma cells. *Metabolomics, 4*, 347–356. https://doi.org/10.1007/s11306-008-0125-3.

Beckonert, O., et al. (2010). High-resolution magic-angle-spinning NMR spectroscopy for metabolic profiling of intact tissues. *Nature Protocols, 5*, 1019–1032. https://doi.org/10.1038/nprot.2010.45.

Bluml, S., Seymour, K. J., & Ross, B. D. (1999). Developmental changes in choline- and ethanolamine-containing compounds measured with proton-decoupled (31)P MRS in in vivo human brain. *Magnetic Resonance in Medicine, 42*, 643–654.

Brown, G. K., Otero, L. J., LeGris, M., & Brown, R. M. (1994). Pyruvate dehydrogenase deficiency. *Journal of Medical Genetics, 31*, 875–879.

Dieterle, F., Ross, A., Schlotterbeck, G., & Senn, H. (2006). Probabilistic quotient normalization as robust method to account for dilution of complex biological mixtures. Application in 1H NMR metabonomics. *Analytical Chemistry, 78*, 4281–4290. https://doi.org/10.1021/ac051632c.

DiMauro, S. (2004). Mitochondrial diseases. *Biochimica et Biophysica Acta, 1658*, 80–88. https://doi.org/10.1016/j.bbabio.2004.03.014.

Diserens, G., et al. (2017). Metabolic stability of cells for extended metabolomical measurements using NMR. A comparison between lysed and additionally heat inactivated cells. *Analyst, 142*, 465–471. https://doi.org/10.1039/c6an02195f.

Gropman, A. L. (2013). Neuroimaging in mitochondrial disorders. *Neurotherapeutics, 10*, 273–285. https://doi.org/10.1007/s13311-012-0161-6.

Harper, A. E., Miller, R. H., & Block, K. P. (1984). Branched-chain amino acid metabolism. *Annual Review of Nutrition, 4*, 409–454. https://doi.org/10.1146/annurev.nu.04.070184.002205.

Jansen, P. H., van der Knaap, M. S., & de Coo, I. F. (1996). Leber's hereditary optic neuropathy with the 11 778 mtDNA mutation and white matter disease resembling multiple sclerosis: Clinical, MRI and MRS findings. *Journal of the Neurological Sciences, 135*, 176–180.

Johnson, M. T., Yang, H. S., & Patel, M. S. (2000). Targeting E3 component of alpha-keto acid dehydrogenase complexes. *Methods in Enzymology, 324*, 465–476.

Kirby, D. M., Crawford, M., Cleary, M. A., Dahl, H. H., Dennett, X., & Thorburn, D. R. (1999). Respiratory chain complex I deficiency: An underdiagnosed energy generation disorder. *Neurology, 52*, 1255–1264.

Koopman, W. J., Distelmaier, F., Smeitink, J. A., & Willems, P. H. (2013). OXPHOS mutations and neurodegeneration. *EMBO Journal, 32*, 9–29. https://doi.org/10.1038/emboj.2012.300.

Koopman, W. J., Willems, P. H., & Smeitink, J. A. (2012). Monogenic mitochondrial disorders. *New England Journal of Medicine, 366*, 1132–1141. https://doi.org/10.1056/NEJMra1012478.

Li, T., et al. (2017). Defective branched-chain amino acid catabolism disrupts glucose metabolism and sensitizes the heart to ischemia-reperfusion injury. *Cell Metabolism, 25*, 374–385. https://doi.org/10.1016/j.cmet.2016.11.005.

Li, Y., et al. (2016). PDHA1 gene knockout in prostate cancer cells results in metabolic reprogramming towards greater glutamine dependence. *Oncotarget, 7*, 53837–53852. https://doi.org/10.18632/oncotarget.10782.

Loeffen, J. L., et al. (2000). Isolated complex I deficiency in children: Clinical, biochemical and genetic aspects. *Human Mutation, 15*(200002), 123–134.

Lynch, C. J., & Adams, S. H. (2014). Branched-chain amino acids in metabolic signalling and insulin resistance. *Nature Reviews Endocrinology, 10*, 723–736. https://doi.org/10.1038/nrendo.2014.171.

Marroquin, L. D., Hynes, J., Dykens, J. A., Jamieson, J. D., & Will, Y. (2007). Circumventing the Crabtree effect: Replacing media glucose with galactose increases susceptibility of HepG2 cells to mitochondrial toxicants. *Toxicological Sciences, 97*, 539–547. https://doi.org/10.1093/toxsci/kfm052.

Mastorodemos, V., Zaganas, I., Spanaki, C., Bessa, M., & Plaitakis, A. (2005). Molecular basis of human glutamate dehydrogenase regulation under changing energy demands. *Journal of Neuroscience Research, 79*, 65–73. https://doi.org/10.1002/jnr.20353.

Mitochondrial Medicine Society's Committee on, D., et al. (2008). The in-depth evaluation of suspected mitochondrial disease. *Molecular Genetics and Metabolism, 94*, 16–37. https://doi.org/10.1016/j.ymgme.2007.11.018.

Moestue, S., Sitter, B., Bathen, T. F., Tessem, M. B., & Gribbestad, I. S. (2011). HR MAS MR spectroscopy in metabolic characterization of cancer. *Current Topics in Medicinal Chemistry, 11*, 2–26.

Morvan, D., & Demidem, A. (2018). NMR metabolomics of fibroblasts with inherited mitochondrial Complex I mutation reveals treatment-reversible lipid and amino acid metabolism alterations. *Metabolomics, 14*, 55. https://doi.org/10.1007/s11306-018-1345-9.

Nicholson, J. K., Lindon, J. C., & Holmes, E. (1999). 'Metabonomics': understanding the metabolic responses of living systems to pathophysiological stimuli via multivariate statistical analysis of biological NMR spectroscopic data. *Xenobiotica, 29*, 1181–1189. https://doi.org/10.1080/004982599238047.

Robinson, B. H. (1998). Human complex I deficiency: Clinical spectrum and involvement of oxygen free radicals in the pathogenicity of the defect. *Biochimica et Biophysica Acta, 1364*, 271–286.

Robinson, B. H., MacKay, N., Chun, K., & Ling, M. (1996). Disorders of pyruvate carboxylase and the pyruvate dehydrogenase complex. *Journal of Inherited Metabolic Diseases, 19*, 452–462.

Robinson, B. H., Petrova-Benedict, R., Buncic, J. R., & Wallace, D. C. (1992). Nonviability of cells with oxidative defects in galactose medium: A screening test for affected patient fibroblasts. *Biochemical Medicine and Metabolic Biology, 48*, 122–126.

Rossignol, R., Gilkerson, R., Aggeler, R., Yamagata, K., Remington, S. J., & Capaldi, R. A. (2004). Energy substrate modulates mitochondrial structure and oxidative capacity in cancer cells. *Cancer Research, 64*, 985–993.

Smeitink, J. A. (2003). Mitochondrial disorders: Clinical presentation and diagnostic dilemmas. *Journal of Inherited Metabolic Diseases, 26*, 199–207.

Smeitink, J. A., Zeviani, M., Turnbull, D. M., & Jacobs, H. T. (2006). Mitochondrial medicine: A metabolic perspective on the pathology of oxidative phosphorylation disorders. *Cell Metabolism, 3*, 9–13. https://doi.org/10.1016/j.cmet.2005.12.001.

Udhane, S. S., et al. (2017). Combined transcriptome and metabolome analyses of metformin effects reveal novel links between metabolic networks in steroidogenic systems. *Scientific Reports, 7*, 8652. https://doi.org/10.1038/s41598-017-09189-y.

Vafai, S. B., & Mootha, V. K. (2013). Medicine. A common pathway for a rare disease? *Science, 342*, 1453–1454. https://doi.org/10.1126/science.1248449.

Vermathen, M., Diserens, G., Vermathen, P., & Furrer, J. (2017). Metabolic profiling of cells in response to drug treatment using (1) H high-resolution magic angle spinning (HR-MAS) NMR spectroscopy. *Chimia, 71*, 124–129. https://doi.org/10.2533/chimia.2017.124.

Vermathen, M., Paul, L. E., Diserens, G., Vermathen, P., & Furrer, J. (2015). 1H HR-MAS NMR based metabolic profiling of cells in response to treatment with a hexacationic ruthenium metallaprism as potential anticancer drug. *PLoS ONE, 10*, e0128478. https://doi.org/10.1371/journal.pone.0128478.

Wishart, D. S., et al. (2013). HMDB 3.0—the human metabolome database in 2013. *Nucleic Acids Research, 41*, D801–D807. https://doi.org/10.1093/nar/gks1065.

Yang, C., et al. (2014). Glutamine oxidation maintains the TCA cycle and cell survival during impaired mitochondrial pyruvate transport. *Molecular Cell, 56*, 414–424. https://doi.org/10.1016/j.molcel.2014.09.025.

Zhou, X., & Thompson, J. R. (1996). Regulation of glutamate dehydrogenase by branched-chain amino acids in skeletal muscle from rats and chicks. *The International Journal of Biochemistry and Cell Biology, 28*, 787–793.